STN area detection using K-NN classifiers for MER recordings in Parkinson patients during neurostimulator implant surgery

L Schiaffino[1], A Rosado Muñoz[2] , J Guerrero Martínez[2] , J Francés Villora[2], A Gutiérrez[3], I Martínez Torres[3] y D R Kohan[4]

[1] Rehabilitation Engineering and Neuromuscular and Sensorial Research Laboratory (LIRINS) of the National University of Entre Ríos, Argentine.
[2] Digital Signal Processing Group, ETSE, Department of Electronic Engineering, University of Valencia, Valencia, Spain.
[3] Functional Neurosurgery Unit. La Fe Hospital, Valencia, Spain.
[4] Chair of Probability and Statistics of the Faculty of Engineering of the National University of Entre Ríos, Argentine.

E-mail: lschiaffino@bioingenieria.edu.ar

Abstract. Deep Brain Stimulation (DBS) applies electric pulses into the subthalamic nucleus (STN) improving tremor and other symptoms associated to Parkinson's disease. Accurate STN detection for proper location and implant of the stimulating electrodes is a complex task and surgeons are not always certain about final location. Signals from the STN acquired during DBS surgery are obtained with microelectrodes, having specific characteristics differing from other brain areas. Using supervised learning, a trained model based on previous microelectrode recordings (MER) can be obtained, being able to successfully classify the STN area for new MER signals. The K Nearest Neighbours (K-NN) algorithm has been successfully applied to STN detection. However, the use of the fuzzy form of the K-NN algorithm (KNN-F) has not been reported. This work compares the STN detection algorithm of K-NN and KNN-F. Real MER recordings from eight patients where previously classified by neurophysiologists, defining 15 features. Sensitivity and specificity for the classifiers are obtained, Wilcoxon signed rank non-parametric test is used as statistical hypothesis validation. We conclude that the performance of KNN-F classifier is higher than K-NN with $p<0.01$ in STN specificity.

1. Introduction

Deep Brain Stimulation (DBS) is an effective neurosurgery to overcome motor system alterations such as tremors, rigidity and dyskinesia appearing in advanced stages of the Parkinson's disease [1][2]. Stimulating DBS electrodes can be implanted in some brain basal nucleus, being the sub-thalamic nucleus (STN) which has proven a better clinical response in implanted patients [1]. An X-ray picture of a patient with implanted DBS electrodes is shown in figure 1. The STN is a small lens-shaped nucleus with an approximated size of 5.9[mm]×3.7[mm]×5[mm] located in the transition between the diencephalon and mesencephalon surrounded by other structures functionally called substantia nigra, red nucleus and zona incerta area [3].

An implanted DBS system acts as a brain pacemaker, generating electrical impulses specifically tuned for each patient for a better motor system response. Typically, the stimulation parameters are [1]: 2[V] biphasic rectangular pulse with a pulse width of 60 [μs] at a frequency of 130 [Hz].

The detection of the target area to fix the stimulation electrodes in the STN is a complex task performed by the neurosurgery team. Depending on the available technology at an institution, the surgeons can be assisted by different tools: previous magnetic resonance to surgery, generic atlas overlapped to obtained images, tomography images during surgery, 3D reconstruction for the fusion of resonance and tomography images (coregister), visual and acoustic analysis of MER acquired signals [2][4][5]. Microelectrodes are 100μm in diameter entering the brain by means of a mechanical system, crossing different brain functional structures as seen on figure 1 (left): anterior thalamus (TH), zona incerta area (ZI), STN and substantia nigra (SN). Each of the functional areas are characterized by different signal patterns [2]. Signals acquired from MER are non-stationary and they are formed by trigger sequences coming from: i) neural activity in form of spikes, ii) background neural activity and iii) artifacts [2].

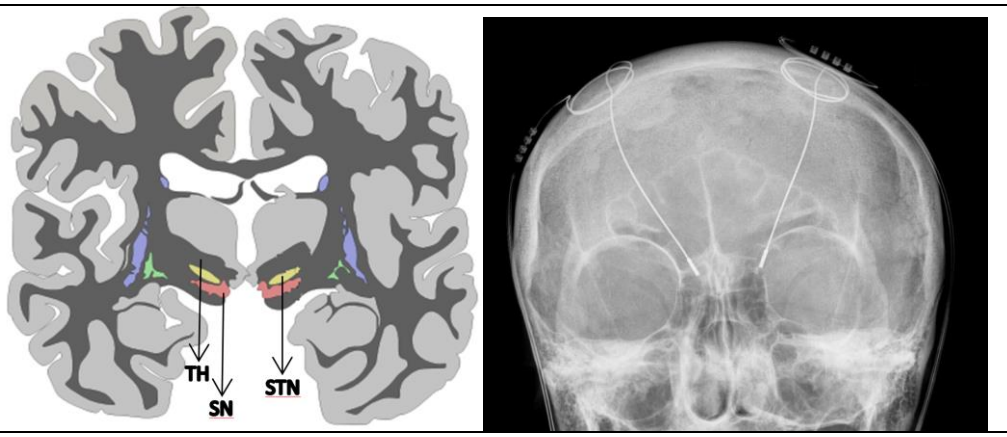

Figure 1. Left: Basal nuclei in the brain: Thalamus-TH, Subthalamus-STN and Substantia nigra-SN. Right: X-ray picture of a patient with a bilateral DBS implant.

Data mining tools are a useful to generate a model. Based on supervised learning and using previously acquired recordings, the model can successfully classify the STN area in new MER recordings. Guillen P. et al [6] were able to discriminate four sub-cortical zones (classes) in MER using statistical indexes further classified by 4.5 decision trees. However, it was robust but did not achieved a good precision in classification. Rodriguez – Sanchez A. et al [7] used non-linear indexes (correlation dimension, Hurst exponent and Lyapunov exponent) obtained from MER. The authors concluded that similar classification ratios could be achieved from statistical indexes than those obtained by non-linear indexes. Ciecierski K. et al [3] used decision trees to evaluate the Euclidean distance and the minimum variance algorithm to classify the mean square value into three groups: background noise amplitude, lowest and highest frequency in the background noise (calculated by means of the discrete Wavelet transform), and correlation between the pair of electrodes existing in the recording. The authors conclude that using these indicators is more stable and less statistically dependent than using spike detection. In addition, they show low classification ratios for some brain areas. Art Chaovalitwongse W. et al [2] propose three classifiers: Naive Bayes, K-nearest neighbours (K-NN) and decision tree using 13 statistical features and one frequency indicator obtained from the MER signals. They show that results obtained using the frequency indicator are poor and statistical features show better performance. From the three proposed classifiers, those obtaining better ratios were the decision tree and K-NN, achieving a sensitivity and specificity around 80% for the STN brain area. Up to our knowledge, there are no results for STN classification using Fuzzy K-NN (KNN-F) which improves the results of K-NN. This work describes STN detection using MER signals and comparing results between K-NN and KNN-F

classifiers. Section 2 describes the methodology of the analysis and used data, followed by section 3 where the classification results are described. Finally, section 4 provides the discussion of the obtained results and the conclusions.

2. Methodology

2.1. Data recordings

La Fe Hospital in Valencia (Spain) leads a DBS implant program for Parkinson patients not responding to drugs. This study analyses MER neural activity recordings acquired from 8 patients during bilateral DBS surgery to implant the DBS stimulator in the STN area. Previously to surgery, the surgeons' team define the MER insertion trajectory supported by magnetic resonance images. This image also allows to define the target area where the stimulation electrode must be implanted. The surgery technique used at La Fe Hospital acquires tomography images at the time of surgery, which are merged with the initial resonance image (coregister) so that the position of the stimulation electrode can be accurately determined and finally positioned in the STN. Moreover, neurophysiologists analyse the electrical signal from MER during all the trajectory to evaluate the area where the electrodes are located in the brain: TH, STN or SN. This signal analysis allows to settle the start and the end of the STN area and they can even define the best position inside the STN according to the electrical signal patterns. In this work, the nerula activity recording was made in both brain hemispheres with 2 parallel MER electrodes per hemisphere (2 [mm] separation) using a Medtronic recorder model 3389 with platinum-iridium electrodes and an impedance between 2 and 6 [MOhm] at 1000 [Hz]. Recordings were obtained at 12 [kHz] sampling frequency using a 16-bit A/D converter at a total gain of 10000x with a 50 [Hz] mains filter. All recording were acquired with the MicroGuide Pro™ system from Alpha Omega which also determines the MER distance from the target area.

Data recording was done from 7 [mm] before to 4 [mm] after the target area. The MER advance was fixed in 0.2 [mm] steps with 1 second acquisition time in each step. Thus, 220 1-second registers was obtained from each patient. All recordings were later marked as in TH, STN or SN areas by the neurophysiologists and also validated by the acquired coregister images.

2.2. MER features obtained from recordings.

Signal processing was done in 1-second windows to calculate 15 features using Matlab®. Those registers showing artifacts and/or very low signal amplitude were discarded. For the remaining valid registers, the obtained parameters were, according to [2][4]:

1. Spike-independent features:
   - basal: Basal amplitude value assessing the envolvent using the Hilbert transform.
   - kurt: Signal kurtosis.
   - CL: Sum of absolute value for the signal derivative.
   - TH: Threshold in the signal amplitude.
   - PK: Peaks number.
   - RA: RMS value of amplitude.
   - NE Non-linear mean energy.
   - ZC: Zero crossings.

2. Spike-dependent features:
   - SBI: Ratio between the number of interspike time intervals lower than 10 [ms] and intervals higher than 10 [ms].
   - SP (pause ratio): Ratio between the number of interspike time intervals higher than 50 [ms] and intervals lower than 50 [ms].
   - SPR (pause index ratio): Ratio between the accumulated interspike time in a time higher and lower than 50 [ms].

- SC: Spikes per second.
- SMAD: Mean spike differential amplitude as the mean value for the amplitude in two consecutive spikes.
- SSD: Standard deviation of interspike intervals.
- SF: Mean spike trigger frequency.

Thus, a signal database with all 15 parameters for each insertion step, MER electrode and patient was created, including the zone annotation class (TH, STN or SN) given by neurophysiologists. In case of zero or undetermined value of all parameters in a certain insertion step value, this step was removed from the database. As classifiers must have balanced register values in each class, 50 registers for each zone and patient were taken. Finally, the dataset was scaled between [0,1].

2.3. K nearest neighbours classifier (K-NN)

Let $R(z) \subset \Re^N$ a hypersphere with V volume centred in z. N_k is the number of samples for a training dataset T_k for the K-NN classifier and w_k the assigned class. The probability of having exactly n samples inside R(z) has a binomial distribution [8] according to equation (1).

$$E[n] = N_k \int_{y \in R(z)} p(y \mid w_k) dy \approx N_k V_{p(y|w_k)} \tag{1}$$

If a certain radius is chosen around z, able to generate a volume exactly containing K samples, then, the radius and its volume depends on the z position inside the measurement space [8]. Thus, we can describe V(z) instead of V, being the estimation of the density [9] that in equation (2).

$$\hat{p}(z|w_k) = \frac{K}{N_k V(z)} \tag{2}$$

In K-NN, the value of K is fixed to estimate the model and the minimum volume V(z) containing those K samples [9]. Expression in equation (2) shows that, in regions where the density estimation is high, a low volume is expected. This is similar to a reduced interpolation zone. On the other hand, when the density estimation is low, the sphere has to grow in size to include all samples [9].

Parameter K controls the balance between the observational error and the variance according to equation (3) [8].

$$\begin{aligned} &k \to \infty \quad \text{and} \quad N_k \to \infty \text{ to obtain a low variance} \\ &k / N_k \to 0 \quad \text{and} \quad N_k \to \infty \text{ to obtain a low observational error} \end{aligned} \tag{3}$$

The K-NN technique has a practical interest as it works with the data sample required to estimate the model without calculating the probability density. Being K_k the number of neighbour samples from class w_k, then, a conditional density estimator can be described in equation (4).

$$\hat{p}(z|w_k) \approx \frac{K_k}{N_k V(z)} \tag{4}$$

Combining (4) with the Naive Bayes classifier with uniform cost function [8], the estimated classification is obtained in equation (5).

$$\begin{aligned} &\hat{w}(z) = w_k \\ &k = \arg\max_{i=1,\ldots,K} \left\{ \hat{p}(z|w_i) \hat{P}(w_i) \right\} = \arg\max_{i=1,\ldots,K} \left\{ \frac{K_i}{N_i V(z)} \frac{N_i}{N_s} \right\} = \arg\max_{i=1,\ldots,K} \{K_i\} \end{aligned} \tag{5}$$

Expression in equation (5) concludes that the assigned class to vector z is that with the highest number of neighbour samples from class w_k. closest to z. The K-NN method can be implemented with a relatively low computational cost even in case of high data samples [9]. The method greatly depends

on the number of data samples but using the distance (typically Euclidean distance) as the parameter defining the class, a sub-optimal results might be obtained [8]. It is also a classifier which is very sensitive to noise in training data [9]. This work used PRTool under Matlab®; cross correlation (n=10) of training data gave a K value ranging from 1 to 15. Finally, K=3 was adopted as it provided the best performance in the classification for the database. This K value was already used in [2] for similar data as those used in this work.

2.4. Fuzzy K-NN classifier (KNN-F).

This variant of K-NN includes fuzzy logic and this fact allows a sample to obtain a certain degree of pertinence to different classes. Different application of fuzzy K-NN has been reported [10-12]. This method assigns distance functions from the k nearest neighbours to the sample. This method uses the same principle used in K-NN in which the chosen class for a sample is assigned by observing the neighbours with a higher degree of pertinence. Then, the final decision is more precise than K-NN where only distances were compared, especially in overlapped classes [12].

Being $W=\{x_1,\ldots,x_n\} \in \Re^N$ the set of n labelled data samples pertaining to c classes $W=\{Z_1,\ldots,Z_c\}$ where $\mu_i(x)$ (equation 6) is the membership function to be calculated for the input vector, and μ_{ij} is the membership function of the i-th class to vector j of labelled samples [11].

$$\mu_i(x) = \frac{\sum_{j=1}^{k} \mu_{ij}\left(1/\left|x - x_j\right|^{2/(m-1)}\right)}{\sum_{j=1}^{k} 1/\left|x - x_j\right|^{2/(m-1)}} \quad \text{where } i = 1,\ldots,c \tag{6}$$

The degree of pertinence of a sample to one of the classes is influenced by the inverse of the distances to the neighbours. This inverse of the distances can be used as a weight. In equation (6), *m* is the exponential weight representing the importance given to the centre due to the fact of being closer to the sample. Using cross correlation (n=10) of training data, the optimal *m* value ranging between 1 and 10 was obtained. Finally, *m* =2 was fixed as the best classification results were obtained. The nearest neighbour x_k related to the centre Z_i, is more influent when the membership degree is reflected. Assessing the membership degree is a certainty factor to assign a simple to a class. In this work, the KNN-F classifiers were obtained using Matlab®.

2.5. Performance of classifiers

Eight subsets (training and validation) were generated from the total features obtained from the MER recordings (section 2.2). As an example, subset 1 was created with all data from patient 1 (150 registers) for validation and all the other patients from 2 to 8 were used for training (1050 registers). This methodology was repeated for every patient as proposed in [2]. Using the 8 training subsets, 8 K-NN and 8 KNN-F classifiers were obtained, further obtaining the classifier performance for the validation data using a 3x3 confusion matrix. From all the 8 confusion matrices obtained for each classifier, 2 performance indexes were calculated: sensitivity and specificity. Sensitivity represents the ratio of registers detected in the right zone according to the annotated class. These values are shown in the diagonal values of the confusion matrix. Specificity shows those registers not belonging to a zone and they were not classified in that zone. The statistical analysis of the performance values was done using the Wilcoxon signed Rank non-parametric test for paired samples [8]. The tools used to obtain these values were PRTool and Matlab® statistical toolbox.

3. Results

Table 1 shows the results of sensitivity and specificity for the TH zone obtained with the two proposed classifiers (K-NN and KNN-F) using 15 features. The Wilcoxon signed rank test show $p<0.01$ for sensitivity and $p<0.05$ for specificity in the TH zone. In Figure 2 the box plot for both classifiers can be seen in the HT zone.

Table 1. Sensitivity and specificity for the TH zone using the K-NN and KNN-F classifiers trained with 15 features.

	Sensitivity K-NN	Sensitivity KNN-F	Specificity K-NN	Specificity KNN-F
Validation 1	0.73	0.85	0.79	0.91
Validation 2	0.76	0.82	0.80	0.89
Validation 3	0.73	0.88	0.69	0.91
Validation 4	0.73	0.86	0.83	0.93
Validation 5	0.66	0.86	0.71	0.90
Validation 6	0.71	0.91	0.77	0.94
Validation 7	0.72	0.86	0.84	0.84
Validation 8	0.79	0.84	0.71	0.84
Average	**0.73±0.038**	**0.86±0.027**	**0.77±0.058**	**0.90±0.037**

Table 2 shows the results of sensitivity and specificity for the STN zone obtained with the classifiers K-NN and KNN-F using 15 features. The Wilcoxon signed rank test shows a non-significant difference for sensitivity and $p<0.01$ for specificity in the STN zone. In Figure 3 the box plot for both classifiers can be seen in the STN zone.

Table 3 shows the results of sensitivity and specificity for the SN zone obtained with the proposed classifiers using 15 characteristics. The Wilcoxon signed rank test shows $p<0.05$ for sensitivity and non-significant difference in specificity in SN zone. In figure 4 the box plot for both classifiers can be seen in the SN zone.

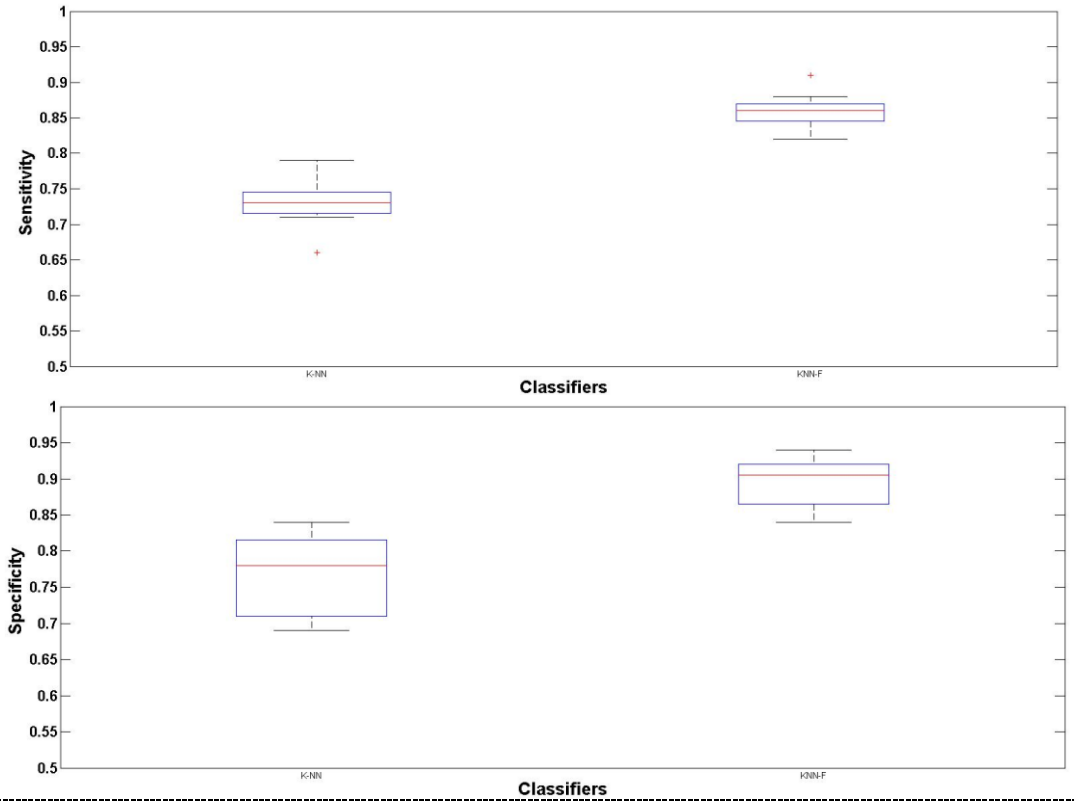

Figure 2. Sensitivity boxes diagrams (top) and specificity (below) for TH zone using the K-NN and KNN-F classifiers trained with 15 features.

Table 2. Sensitivity and specificity for the STN zone using the K-NN and KNN-F classifiers trained with 15 features.

	Sensitivity K-NN	Sensitivity KNN-F	Specificity K-NN	Specificity KNN-F
Validation 1	0.62	0.72	0.75	0.82
Validation 2	0.80	0.84	0.37	0.82
Validation 3	0.68	0.77	0.62	0.73
Validation 4	0.59	0.69	0.73	0.91
Validation 5	0.70	0.70	0.68	0.86
Validation 6	0.69	0.71	0.74	0.78
Validation 7	0.75	0.64	0.70	0.75
Validation 8	0.84	0.67	0.65	0.89
Average	**0.71±0.085**	**0.72±0.062**	**0.66±0.124**	**0.82±0.065**

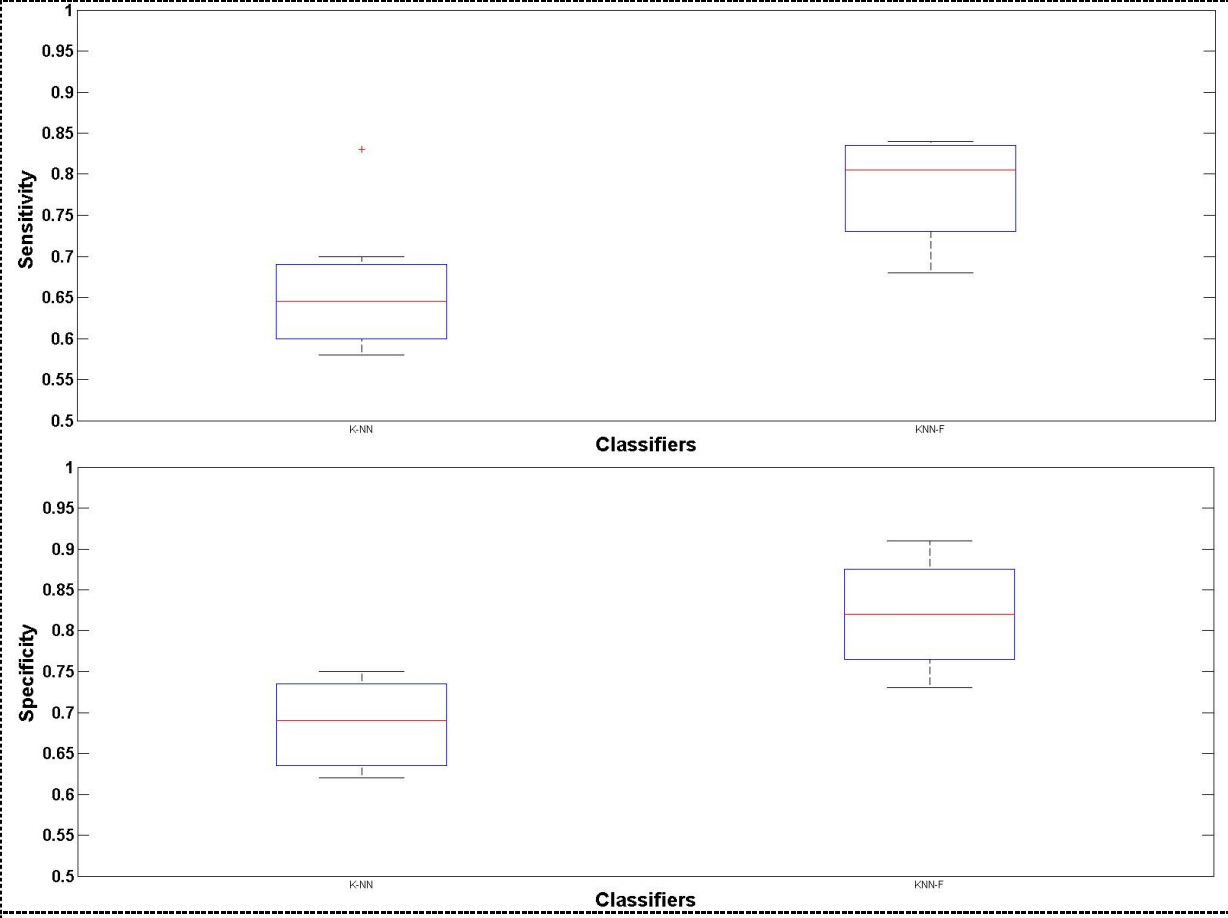

Figure 3. Sensitivity boxes diagrams (top) and specificity (below) for STN zone using the K-NN and KNN-F classifiers trained with 15 features.

Table 3. Sensitivity and specificity for the SN zone using the K-NN and KNN-F classifiers trained with 15 features.

	Sensitivity K-NN	Sensitivity KNN-F	Specificity K-NN	Specificity KNN-F
Validation 1	0.68	0.81	0.56	0.73
Validation 2	0.58	0.68	0.71	0.75
Validation 3	0.83	0.83	0.64	0.80
Validation 4	0.65	0.80	0.85	0.73
Validation 5	0.70	0.84	0.67	0.78
Validation 6	0.64	0.84	0.65	0.82
Validation 7	0.62	0.77	0.73	0.66
Validation 8	0.41	0.69	0.69	0.76
Average	**0.64±0.118**	**0.78±0.065**	**0.68±0.084**	**0.75±0.05**

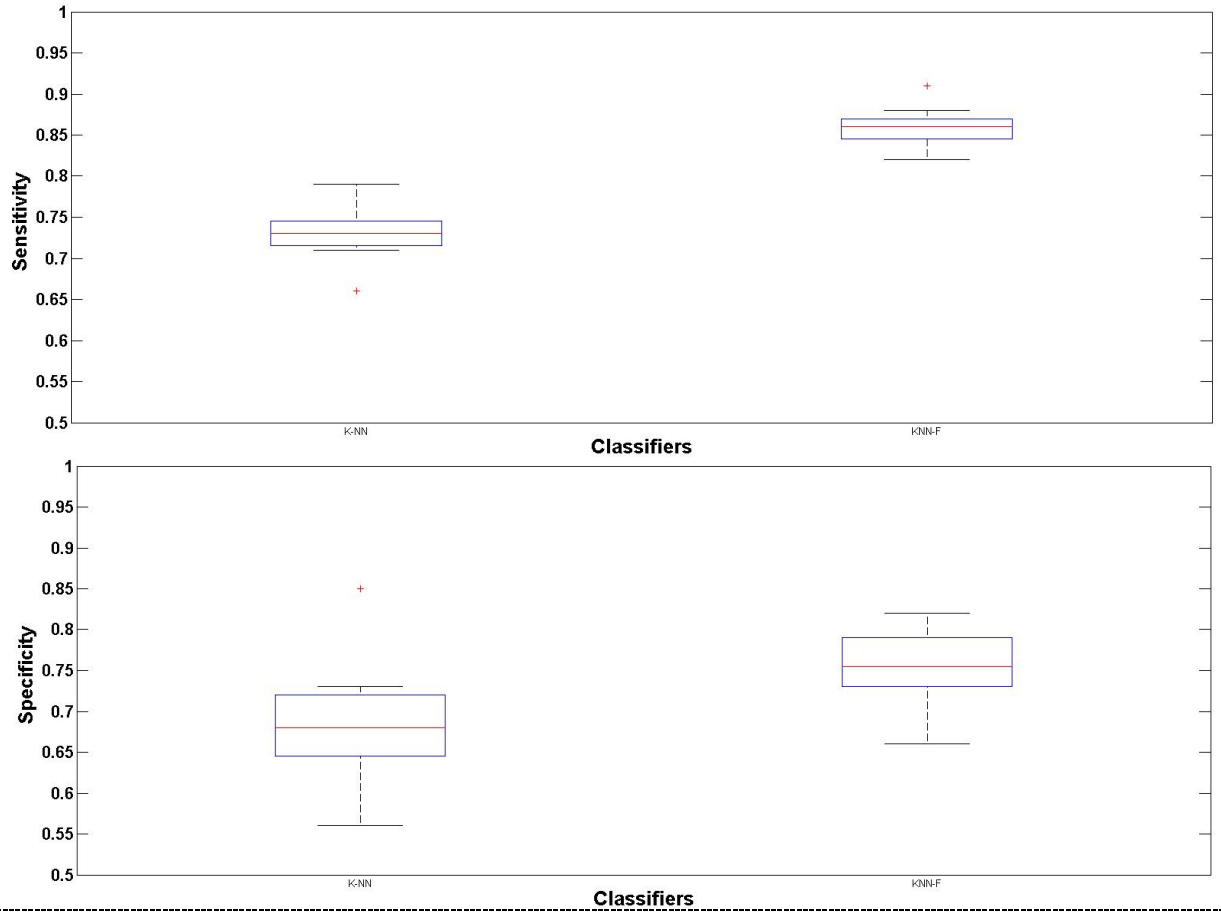

Figure 4. Sensitivity boxes diagrams (top) and specificity (below) for SN zone using the K-NN and KNN-F classifiers trained with 15 features.

4. Discussion and conclusions

The analysis of the results shows that the classifier KNN-F has better performance in all zones of classification. Specifically it has a very significant difference in sensitivity in the TH zone and significant difference in sensitivity of SN zone. For the zone of interest, that is the STN zone, the average sensitivity results were 0.72 ± 0.062 and average specificity results were 0.82 ± 0.065. Although we can not ensure a significant difference for sensitivity between the two methods, the statistical study shows a very significant difference in specificity. Probably it can be obtained higher sensitivities and specificities in the zone of interest and significant difference in sensitivity in the KNN zone if the number of patients for training classifiers it is increased. It is concluded that the performance of KNN-F classifier is acceptable and superior than KNN for the experimental conditions of this study and a group of 8 patients. Also it is possible, as a continuation of this work, combine KNN-F obtained by each training set using rules of maximum, minimum and average [10] which would provide a single more robust classifier with higher sensitivity and specificity, as it is proposed by [9] to other classifiers.

5. References

[1] Martínez Torres I Doctoral Thesis. 2014. Optimization and quantification of stimulation parameters in subthalamic nucleus deep brain stimulation for Parkinson's disease. Universidad de Valencia.

[2] Chaovalitwongse W A, Jeong Y-S, Jeong M-K, Danish S F and Wong S 2011 Pattern Recognition Approaches for Identifying Subcortical Targets during Deep Brain Stimulation Surgery *IEEE Intell. Syst.* **26** 54–63

[3] Ciecierski K, Raś Z W and Przybyszewski A W 2012 Foundations of Recommender System for STN Localization during DBS Surgery in Parkinson's Patients *Foundations of Intelligent Systems* Lecture Notes in Computer Science ed L Chen, A Felfernig, J Liu and Z W Raś (Springer Berlin Heidelberg) pp 234–43

[4] Guerrero-Martínez J. R-M A 2015 Characterization of Microelectrode Records in Deep Brain Stimulation Applied to Parkinson's Disease Patients *IFMBE* **49** 647–50

[5] Bronstein J M, Tagliati M, Alterman R L, Lozano A M, Volkmann J, Stefani A, Horak F B, Okun M S, Foote K D, Krack P, Pahwa R, Henderson J M, Hariz M I, Bakay R A, Rezai A, Marks W J, Moro E, Vitek J L, Weaver F M, Gross R E and DeLong M R 2011 Deep brain stimulation for Parkinson disease: an expert consensus and review of key issues *Arch. Neurol.* **68** 165

[6] Guillen P, Argaez M, Martínez-de-Pisón F, Velazquez L and Martinez-de-Pison F 2012 Data mining in the process of localization and classification of subcorticals structures *2012 6th Euro American Conference on Telematics and Information Systems (EATIS)* 2012 6th Euro American Conference on Telematics and Information Systems (EATIS) pp 1–5

[7] Rodriguez-Sanchez A, Delgado-Trejos E, Orozco-Gutierrez A, Castellanos-Dominguez G and Guijarro-Estelles E 2008 Nonlinear Dynamics Techniques for the Detection of the Brain Areas Using MER Signals *International Conference on BioMedical Engineering and Informatics, 2008. BMEI 2008* International Conference on BioMedical Engineering and Informatics, 2008. BMEI 2008 vol 2 pp 198–202

[8] Miner G, Nisbet R and IV J E 2009 *Handbook of Statistical Analysis and Data Mining Applications* (Amsterdam ; Boston: Academic Press)

[9] Heijden F van der, Duin R, Ridder D de and Tax D M J. 2005. Book *Classification, Parameter Estimation and State Estimation: An Engineering Approach Using MATLAB* (John Wiley & Sons)

[10] Piorno Campo J Master Thesis. 2009. Diseño de un nuevo clasificador supervisado para minería de datos. Universidad Complutense de Madrid.

[11] Keller J M, Gray M R and Givens J A 1985 A fuzzy K-nearest neighbor algorithm *IEEE Trans. Syst. Man Cybern.* **SMC-15** 580–5

[12] Kim S-Y, Sim J and Lee J 2006 Fuzzy k-Nearest Neighbor Method for Protein Secondary Structure Prediction and Its Parallel Implementation *Computational Intelligence and Bioinformatics* Lecture Notes in Computer Science ed D-S Huang, K Li and G W Irwin (Springer Berlin Heidelberg) pp 444–53

Acknowledgement
The authors wish to thank the Carolina Foundation, the University of Valencia, the Faculty of Engineering of the National University of Entre Ríos and the Autonomous University of Entre Rios for the aid received for the doctoral scholarship of Ms. Bioing. Luciano Schiaffino. Also thank Functional Neurosurgery Unit of La Fe Hospital (Valencia - Spain) by the advice received.